# Dust concentration distribution and analysis of influencing factors in the heading face of Shangwan coal mine

Yufu Li[1], Jie Wang[1]*, Zhibin Li[2] and Haitao Mo[2]

[1]Shangwan Coal Mine, Ulanmulun Town, Ejin Horo Banner, Ordos, Inner Mongolia Autonomous Region, China, [2]Xi'an Research Institute Co. Ltd., China Coal Technology and Engineering Group Corp., Xi'an, China

Dust concentration in coal mine roadways significantly affects worker safety and health. Effective dust control is critical for optimizing the mine ventilation system and creating a safer working environment. This study investigates the impact of ventilation duct arrangements on dust concentration in a heading face, aiming to identify the optimal configurations for minimizing dust levels and enhancing worker safety. Using numerical simulations based on the gas-solid two-phase flow model in Fluent, we analyzed the effects of varying duct outlet distances and heights on airflow patterns and dust dispersion. Mesh generation, grid independence verification, and detailed parameter settings ensured accuracy and reliability of the simulation results. Results indicate that positioning the duct outlet 8 m from the heading face reduces dust concentration to approximately 39 mg/m$^3$, while setting the duct height at 1.5 m notably decreases dust levels in the worker breathing zone. A mesh density of 576,449 cells ensured convergence and computational efficiency with an error margin within 2%. The findings provide practical insights into ventilation system optimization for coal mine heading faces, contributing to improved occupational health and operational safety. Future research should focus on validating these results through field experiments and addressing complex real-world conditions.

KEYWORDS

dust concentration, dust removal, numerical simulation, coal mine, fluent

## 1 Introduction

In underground metal and non-metal mine heading operations, the use of rock drilling equipment—including drilling, blasting, and loading processes—generates substantial amounts of dust. This dust significantly increases roadway dust concentration and accelerates equipment wear, posing serious threats to worker safety and occupational health (Perret et al., 2017; Zhang et al., 2024; Shekarian et al., 2021). As a result, effective dust control has become a primary concern for the mining industry.

To address this challenge, numerical simulations are increasingly employed as a key approach to developing effective dust control strategies. With advancements in computational fluid dynamics (CFD), numerical methods have been widely adopted to analyze dust transport patterns in roadways, providing insights into effective dust mitigation techniques (Trechera et al., 2021; Liu and Liu, 2020). These methods enable the simulation of complex roadway environments and offer critical theoretical support for practical dust control measures. Commonly used CFD software, such as ANSYS Fluent, ANSYS CFX,

and ShonDY, can simulate the entire dust transport process and visually represent dust concentration distributions throughout the roadway, delivering scientific evidence to inform dust control efforts (Abbasi et al., 2021; Jing et al., 2022a; Lu et al., 2021).
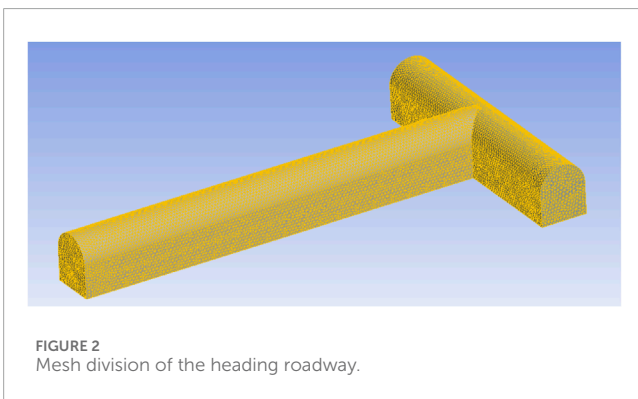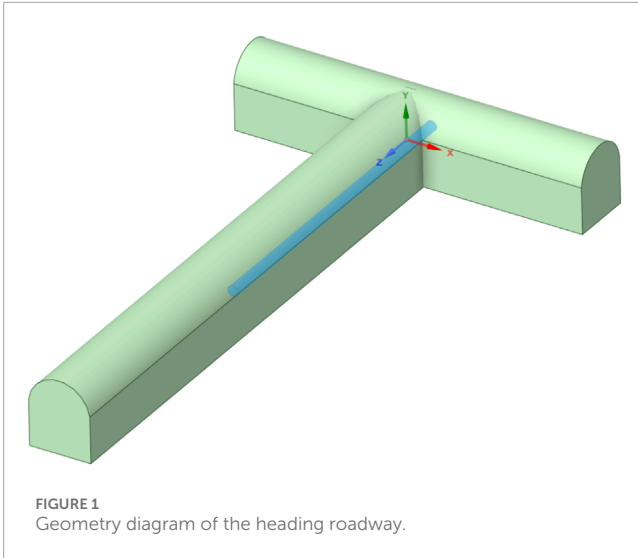
In the study of dust control in coal mine heading roadways, numerical methods have demonstrated unique advantages, particularly in guiding the implementation of on-site dust control measures to effectively identify the most cost-effective solutions. Numerous case studies have validated the practicality and accuracy of numerical simulations. Khan et al. (2022) studied the hazards of coal dust explosibility and methods for its detection, prevention, and control, finding that CFD modeling is an effective tool for evaluating coal dust explosibility. This finding provides a reference for further exploring dust control strategies under different operating conditions. Du et al. (2020) investigated dust migration patterns in the world's highest fully mechanized mining face (8.8 m high), establishing a 1:1 scale model based on field production and conducting qualitative and quantitative analyses of airflow and dust migration through CFD simulations. The results showed that during the movement of the working face, the airflow velocity first increased, then decreased, and then increased again, forming a high dust concentration zone approximately 120 m long with dust concentration exceeding 3,500 mg/m³. This dust migration pattern is common under different mine conditions, providing a foundation for subsequent ventilation and dust removal design optimization. Xiu et al. (2020) studied dust pollution characteristics and optimal dust control airflow rates during coal mine production by establishing a high-fidelity physical model combined with numerical simulations to analyze dust dispersion patterns under different airflow conditions. The results showed that dust mass concentration gradually decreased when the airflow ranged from 700 to 1,600 m³/min, but excessive airflow could cause dust resuspension, polluting the work environment. This study highlights the importance of airflow control in dust management. Zhou et al. (2017) studied the diffusion behavior of respirable dust in a fully mechanized mining face by combining CFD simulations and field measurements to analyze dust migration in the roadway. The results showed that dust produced by the rear drum quickly spread into the pedestrian walkway and further polluted the area under turbulent conditions. This research provides data support for further reducing dust concentration in the working face and protecting worker health. Zhou et al. (2022) studied dust migration patterns under ascending and descending ventilation conditions in fully mechanized mining faces, finding that dust migration distances were longer under ascending ventilation conditions, with the difference in distance increasing over time, providing new ideas for ventilation scheme design. Önder et al. (2009) investigated dust concentration levels in different areas of underground coal mines, finding that production areas had higher dust levels, increasing the risk of respiratory disorders for production workers. Hu et al. (2020) studied the effects of different ventilation velocities on dust dispersion in coal mine roadways, finding that the airflow field could be divided into turbulent, recirculation, and stable zones. When the ventilation velocity exceeded 17 m/s, the dust concentration near the pressure duct outlet and about 5 m behind the roadheader was high, and high ventilation velocities led to dust re-entrainment and increased concentration. By analyzing dust behavior under different airflow conditions, researchers can

better understand the impact of ventilation conditions on dust migration. Zhang et al. (2021) conducted a CFD comparative analysis on the pollution characteristics of coal dust generated by turbulent airflow from coal cutting in the fully mechanized mining face, finding that the turbulence not only increased the intensity of the turbulent flow field but also caused a positive offset in the airflow, increasing the lateral dispersion range of dust in the pedestrian area. However, none of the above researchers conducted further studies on the positioning of the ventilation duct. Dust generation in underground mining operations poses severe occupational health risks and reduces equipment efficiency. The need for effective dust control is paramount, as prolonged exposure to high dust concentrations can result in chronic respiratory illnesses, such as coal workers' pneumoconiosis, and degrade the performance of mining equipment due to abrasive wear. Despite existing guidelines and regulations on mine ventilation and dust control, the dynamic and site-specific nature of underground environments presents significant challenges to achieving optimal dust removal. Addressing this issue requires comprehensive studies to understand the influence of ventilation parameters on dust dispersion. This study is critical for developing scientifically grounded and practical strategies for improving ventilation efficiency and minimizing health hazards in coal mining operations.

Based on the aforementioned research findings, this study uses Space Claim software to construct a three-dimensional model of forced ventilation in the heading roadway and employs Ansys Workbench Meshing software for mesh generation. The data are then imported into Fluent software for simulation. Based on the gas-solid two-phase flow theory and combined with field measurements, the study selected the loader operation site at the 22,106 working face of Shangwan Coal Mine as the research object, as this area has high dust production and continuous worker activity. By simulating different duct heights and the distance between the duct outlet and the heading face, the dust transport patterns were studied, and the optimal position and operational parameters for duct placement at the 22,106 working face of Shangwan Coal Mine were determined, providing strong references for on-site ventilation and dust control.

## 2 Model construction

The research and application project for exhaust ventilation and dust control technology in Shangwan Coal Mine was commissioned by Shendong Coal Co., Ltd., and implemented by China Coal Technology and Engineering Group Xi'an Research Institute Co., Ltd. In conducting numerical simulations using Fluent software, the model was simplified by considering the heading roadway, intake airway, and return airway as standard three-centered arch roadways with smooth surfaces, without any loose rocks, protrusions, or depressions. The computational domain of the model was set to a length of 20 m, with a cross-section of 3.0 m by 3.0 m in a standard three-centered arch shape. Specific parameters include an arch height of 1.0 m and a cross-sectional area of 8.358 square meters. The radius of the larger arch is 2.076 m with an angle of 67.37°, while the radius of the smaller arch is 0.783 m with an angle of 56.32°. The ventilation duct layout was set at different distances from the heading face, specifically at 2 m, 4 m, 6 m, and 8 m. Each duct had a diameter of 400 mm, and the height of the duct bottom from the

FIGURE 1
Geometry diagram of the heading roadway.



FIGURE 2
Mesh division of the heading roadway.



FIGURE 3
Local mesh refinement of the ventilation duct layout.

TABLE 1  Mesh quality analysis results.

| Parameter | Parameter |
|---|---|
| Number of Cells | 576,449 |
| Maximum Cell Size | 0.03 |
| Skewness | Max:0.85 Average: 0.23 |
| Orthogonality | Average: 0.78 |
| Cell Volume Variation Rate | Uniform Distribution |
| Mesh Skewness in Refined Region | <0.5 |

roadway floor was set at 0.5 m, 1 m, 1.5 m, and 2 m, respectively. The overall model design is shown in Figure 1.

# 3 Numerical simulation

## 3.1 Mesh generation

After constructing the 3D model using Space claim, it was imported into Ansys Workbench Meshing for mesh generation, followed by importing the model and mesh data into Fluent software for simulation. Due to the computational complexity of the ventilation duct layout, this study used highly adaptive unstructured meshes for detailed partitioning. In particular, local mesh refinement was applied in the ventilation duct layout region to ensure the accuracy and efficiency of the simulations. The maximum cell size for this mesh was set to 0.3 m, with a total mesh count of 576,449 cells. The maximum skewness value was 0.85, with an average skewness of 0.23, and over 95% of the mesh skewness values were below 0.5, meeting the quality requirements for the calculation. The mesh division of the heading roadway is shown in Figure 2, while the local mesh refinement of the ventilation duct layout is shown in Figure 3.
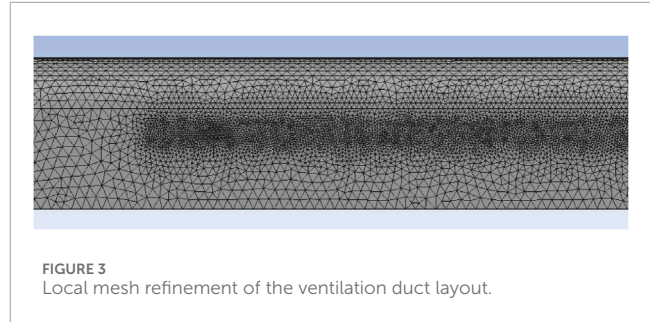
## 3.2 Mesh quality analysis

In numerical simulations, mesh quality is crucial for the convergence of calculations and the accuracy of results. Therefore, a detailed analysis of the mesh quality was conducted to ensure that it meets the requirements for numerical simulation. In this study, Ansys Workbench Meshing was used for a rigorous quality evaluation of the mesh, with the main analysis indicators including skewness, orthogonality, and cell volume variation rate (Lu et al., 2021; Wu et al., 2021; Jing et al., 2022b). Mesh quality results are shown in Table 1.

From Table 1, it can be seen that the mesh division in this study not only involved local refinement in critical regions to improve accuracy but also ensured a high level of overall mesh quality while maintaining a reasonable computational load (Zhou et al., 2015).

## 3.3 Grid independence verification

To ensure the reliability of the numerical simulation results, grid independence verification was conducted (Liu and Feng, 2021; Yang et al., 2021). Grid independence verification involves comparing results obtained with different mesh densities to confirm that the results no longer change significantly with variations in the number of cells, thereby ensuring the accuracy of the calculations, as shown in Figure 4. Coarse, medium-density, and fine meshes were selected for the simulation comparison, with specific cell counts of 350,000, 576,449, and 780,000, respectively. By comparing wind speed and dust concentration parameters at key monitoring points, it was found that the differences between the medium-density and

FIGURE 4
Grid independence verification.
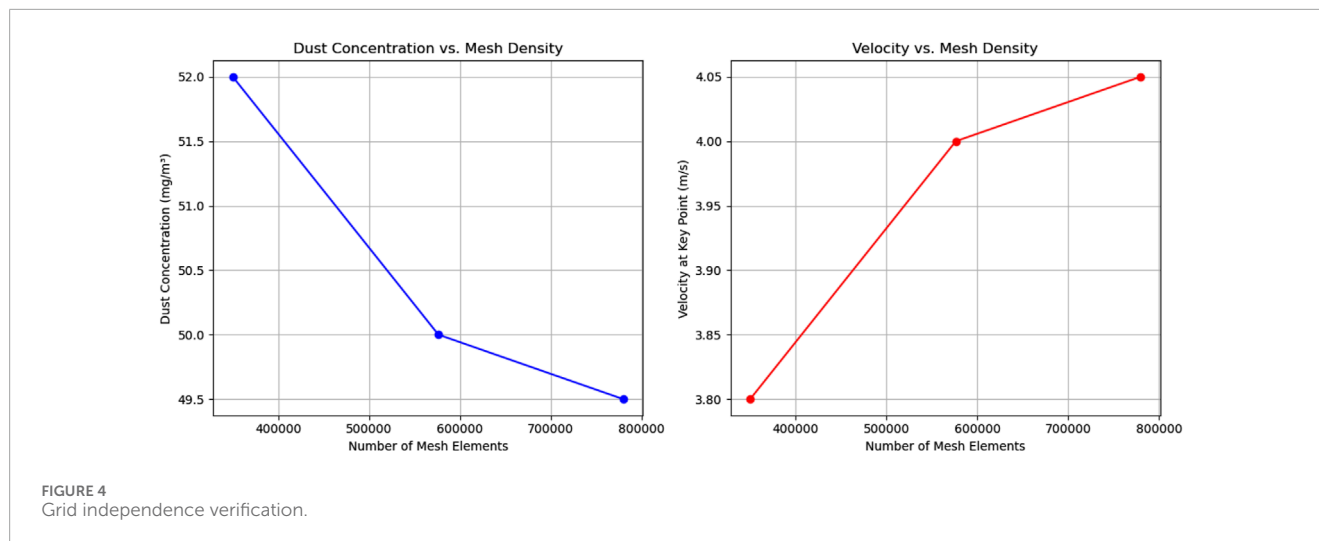
fine mesh results were small, with errors within 2%, and the trends of key parameters remained consistent. In contrast, the results from the coarse mesh showed significant deviations compared to the medium-density and fine meshes, with an error of approximately 8%. To further verify the effect of mesh density on the results, representative locations at the heading face and the middle of the roadway were selected, and dust concentration and wind speed distributions were recorded for different meshes, located at a height of 1 m in the heading roadway, with the ventilation duct positioned 4 m from the working face. The results indicated that when the number of cells increased from 576,449 to 780,000, the changes in the calculated results at each monitoring location were minimal, and the parameter errors were small. Thus, the mesh density of 576,449 cells was considered sufficient to meet the accuracy requirements for this simulation, making it the optimal choice.

Through grid independence verification, it was confirmed that a mesh density of 576,449 cells is sufficient to ensure the accuracy and convergence of the simulation results without the need for further mesh refinement, thereby effectively reducing the consumption of computational resources. The reliability of the grid independence verification results provides a solid foundation for the accuracy of subsequent simulations, ensuring that the model accurately reflects the airflow and dust distribution characteristics.

## 3.4 Solver and boundary condition settings

In the simulation of gas-solid two-phase flow, the Discrete Phase Model (DPM) is employed as the fundamental approach. This method solves the Navier-Stokes equations by defining the fluid as the continuous phase and the solid particles as the discrete phase. The volume fraction of the discrete phase is relatively small, typically less than one-tenth (Chen et al., 2022; Zhou et al., 2023; Geng et al., 2021). Consequently, interactions between discrete particles are generally neglected, and the direct influence of the discrete phase on fluid motion is not considered. However, detailed attention is given to the exchange of momentum, mass, and energy between the continuous and discrete phases.

TABLE 2  Solver parameter settings.

| Parameter index | Parameter settings |
|---|---|
| Solver Type | Pressure-Based Solver |
| Model Type | Discrete Phase Model (DPM) |
| Velocity-Pressure Coupling | SIMPLE Algorithm |
| Volume Fraction Limit | Discrete Phase <10% |
| Iteration Convergence Criterion | $1e^{-4}$ |
| Time Step Settings | Steady-State |
| Turbulence Model | RNG k-ε Model |

The solution parameters and settings are summarized in Table 2, with boundary conditions detailed in Table 3. Additional specific parameters for the dust source and discrete phase are provided in Table 4. This simulation methodology enables researchers to gain an in-depth understanding of the complex interactions between the two phases, even when the discrete phase has a relatively small influence. By leveraging these insights, engineering applications can be optimized, and potential issues can be anticipated, thereby facilitating the development of more effective control strategies for practical operations.

## 4 Simulation results analysis

### 4.1 Velocity flow field analysis

The simulation results were imported into CFD-Post, yielding the distribution of the airflow field and dust distribution at the tunneling working face. To provide a more intuitive observation of the airflow field velocity distribution, velocity contour plots at different heights (0.5 m, 1 m, 1.5 m, and 2 m) in the tunneling

TABLE 3 Boundary conditions.

| Parameter index | Parameter settings |
|---|---|
| Inlet Boundary | Velocity Inlet, Wind Speed of 1 m/s |
| Outlet Boundary | Pressure Outlet, Gauge Pressure of 0 Pa |
| Air Duct Wind Speed (m/s) | 10 |
| Turbulence Intensity (%) | 4.25 (Inflow Tunnel)/4.17 (Air Duct) |
| Hydraulic Diameter (m) | 3.04 (Inflow Tunnel)/0.4 (Air Duct) |
| Wall | No-Slip Wall, Temperature of 300 K |
| Dust Injection Point | Mass Flow Rate of 0.01 kg/s |
| Initial Conditions | Ambient Temperature of 300 K, Static Pressure of 0 Pa |

TABLE 4 Discrete phase parameter settings.

| Parameter index | Parameter settings |
|---|---|
| Dust Source Location | Working Face Area |
| Jet Type | Surface Source |
| Particle Material | Coal Dust, Silicon Dioxide |
| Density (kg/m³) | 2,329.5 |
| Maximum Particle Diameter (m) | 0.0001 |
| Minimum Particle Diameter (m) | 0.000001 |
| Median Particle Diameter (m) | 0.000059 |
| Initial Particle Velocity | Same as Fluid Velocity |
| Momentum Coupling | One-Way Coupling (Zhao et al., 2024) |

roadway were analyzed, as shown in Figure 5. The wind velocity vector diagram for the tunneling roadway at a height of 1.5 m is presented in Figure 6.

Based on the observations from Figures 5, 6, the airflow is ejected at high speed from the air duct outlet directly toward the working face, forming a typical high-speed wall-attached jet flow pattern. This airflow effectively drives dust toward the return air tunnel; however, a portion of the airflow turns near the working face, creating a vortex in this area. This vortex causes localized stagnation, hindering the efficient removal of dust.

This phenomenon highlights that, while part of the airflow successfully transports dust to the return air tunnel, vortex formation near the working face obstructs effective dust control. These findings provide critical insights for optimizing mine ventilation and dust control system design. Future research could explore adjustments to air duct layout, airflow velocity, and direction to enhance dust removal efficiency. By fine-tuning the air duct position and wind speed, a more uniform airflow distribution could

be achieved, reducing vortex formation and improving overall dust control effectiveness. Such optimization would ideally be guided by experimental data and simulation results, ensuring a ventilation system design that is both efficient and economical.

## 4.2 Distance between air duct outlet and working face

According to the "Safety Regulations for Metal and Non-metal Mines" (GB 16423-2020), in a forced ventilation system, the distance between the air duct outlet and the working face must not exceed 10 m (Zhao et al., 2024; Zeqiri et al., 2022). In this study, while keeping the height of the air duct constant, the distance between the air duct outlet and the working face was set to 2 m, 4 m, 6 m, and 8 m for simulation analysis. Additionally, the dust concentration distribution in the worker's operating area 3 m from the working face was recorded, with the specific results shown in Figures 7, 8. Figure 9 shows the average dust concentration distribution across the roadway cross-section at different distances between the air duct outlet and the working face.

As shown in Figures 7, 8, when the air duct outlet is too close to the working face, the dust moves at a higher speed, but the vortex formed by the airflow near the working face causes dust to aggregate and may also trigger secondary dust dispersion. This phenomenon is particularly prominent when the distance between the air duct outlet and the working face is 6 m, where a strong vortex region forms at the outlet, making it difficult for the dust to be removed. In this case, the local dust concentration reaches 50 mg/m³, far exceeding the limit values set by relevant standards.

When the air duct outlet is 8 m from the working face, the working face falls within the optimal jet range, allowing for smoother airflow and rapid dust removal, significantly reducing dust concentration within the roadway. Therefore, maintaining the distance between the air duct outlet and the working face between 8 and 10 m is an appropriate setting. This distance ensures effective jet flow while preventing the formation of vortices, thereby avoiding dust accumulation and secondary dust dispersion.

As illustrated in Figure 9, the different distances between the air duct outlet and the working face have a significant impact on the average dust concentration in the roadway cross-section. If the ventilation parameters are not appropriately selected, the average dust concentration in the roadway can reach as high as 50 mg/m³. As the distance between the air duct outlet and the working face increases, the dust concentration in the roadway gradually decreases. When the distance between the air duct outlet and the working face is 8 m, the dust concentration in the roadway is minimized, achieving the optimal ventilation effect.

## 4.3 Air duct height

With the distance between the air duct outlet and the working face fixed at 8 m and other parameters such as wind speed remaining constant, the height of the air duct was adjusted to 0.5 m, 1 m, 1.5 m, and 2 m for simulation calculations. Simultaneously, the dust concentration distribution in the worker's operating area, 3 m from the working face, was recorded, with the results shown
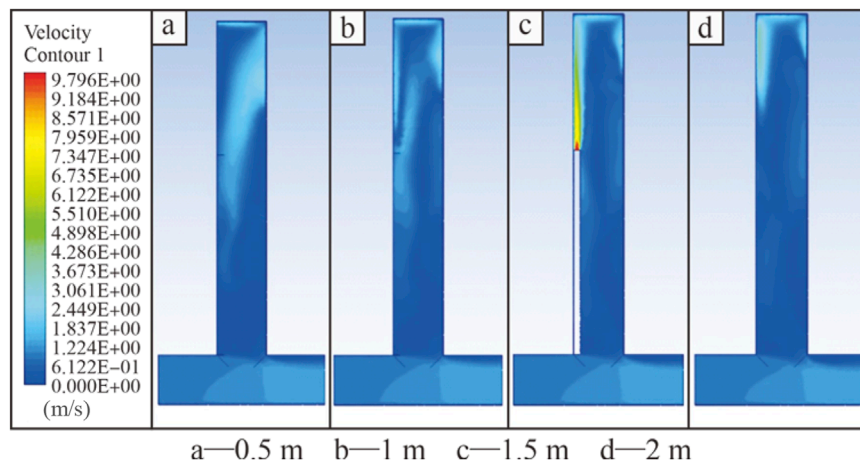
**FIGURE 5**
Velocity contour plot of airflow field at different heights in the tunneling roadway. **(A)** 0.5 m **(B)** 1 m **(C)** 1.5 m **(D)** 2 m.
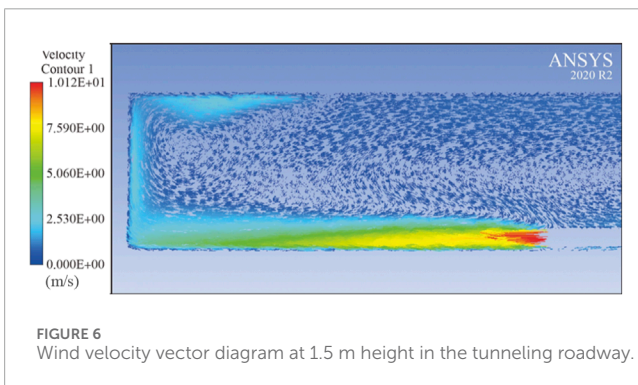


**FIGURE 6**
Wind velocity vector diagram at 1.5 m height in the tunneling roadway.

in Figures 10, 11. In addition, the average dust concentration distribution across the roadway cross-section at different air duct heights is displayed in Figure 12.

As shown in Figures 10, 11, when the air duct is set at a lower height, the airflow ejected from the duct outlet creates vortices in the upper part of the roadway, which carry dust from the bottom of the roadway to the upper areas. This results in an excessively high dust concentration in the upper breathing zone, which is unfavorable for workers' operations. When the air duct is positioned at a height of 1.5 m, although the dust concentration in the local area near the working face is slightly higher compared to the case at 2 m, the overall dust migration speed and dust concentration in the breathing zone are better than those at other heights. This contributes to more effective dust removal during tunneling operations, significantly reducing the dust concentration in the workers' breathing zone and providing a better working environment. Therefore, setting the air duct height at 1.5 m is considered a reasonable choice.

As shown in Figure 12, the trend of dust concentration within the roadway is generally consistent across the four different duct heights. Since the dust source is located at the working face, the average dust concentration is highest at that location. As dust gradually settles within the roadway, the average dust concentration exhibits a declining trend. When the air duct height is set to 1.5 m, the average dust concentration in the roadway is the lowest, indicating that the ventilation effect is optimal at this height.

# 5 Discussion

This study analyzed dust transport behavior during tunneling operations in underground metal and non-metal mines, focusing on the effects of different air duct arrangements through numerical simulations. The results highlight the importance of optimal ventilation configurations in reducing dust concentrations and improving worker safety. While the findings provide practical insights for optimizing mine ventilation systems, several areas require further exploration. The type of ventilation system—direct or diagonal—significantly impacts airflow patterns and dust dispersion. Zeqiri et al. (2022) emphasized that diagonal ventilation systems can effectively distribute airflow when properly regulated, influencing dust control strategies. Similarly, Kurnia et al. (2014) demonstrated the feasibility of intermittent ventilation systems, which reduce energy consumption without compromising safety, offering innovative opportunities for dust control in underground mines. However, this study simplified the model by assuming smooth roadway surfaces and uniform dust particle properties, which may not fully capture real-world complexities. Future research should consider incorporating wall roughness and heterogeneous dust compositions for improved accuracy. Additionally, experimental data integration is essential to validate and refine numerical models, enhancing their applicability. Exploring the effects of air duct arrangements in irregular tunnel geometries and dynamic conditions is also crucial for developing adaptable ventilation solutions. Advanced technologies such as artificial intelligence and machine learning may further enhance simulation accuracy and enable intelligent mine ventilation system design. These directions would build upon the current findings, contributing to safer and more efficient underground working environments.
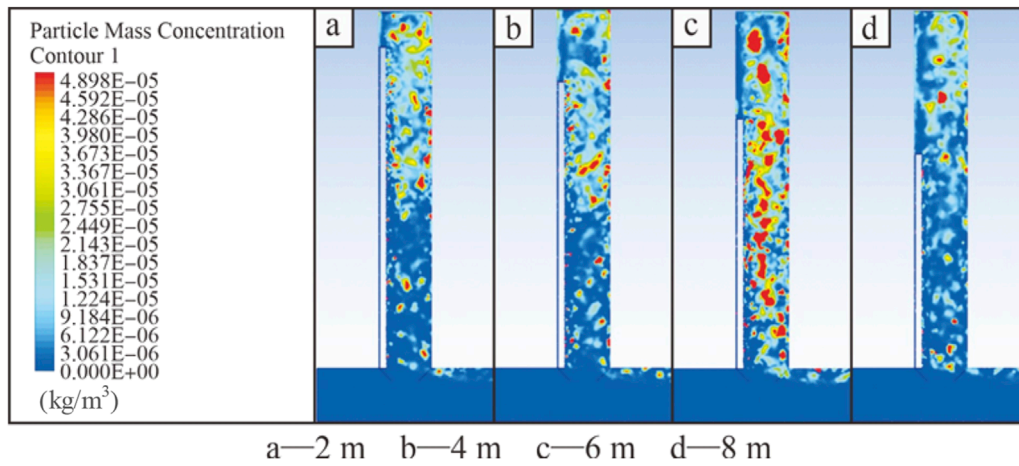
**FIGURE 7**
Wind velocity vector diagram at 1.5 m height in the tunneling roadway. **(A)** 2 m **(B)** 4 m **(C)** 6 m **(D)** 8 m.
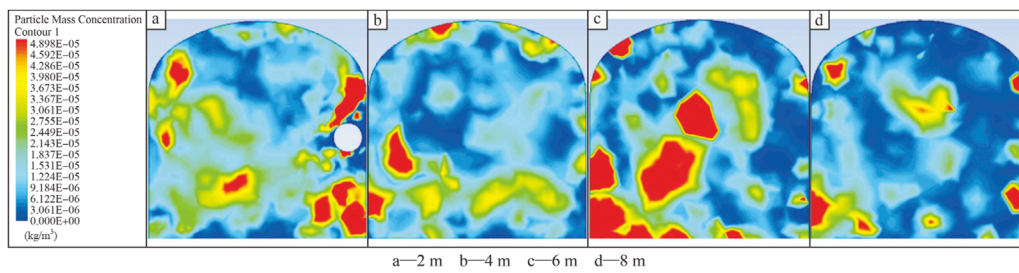


**FIGURE 8**
Dust concentration distribution 3 m from the working face at different distances between the air duct outlet and the working face. **(A)** 2 m **(B)** 4 m **(C)** 6 m **(D)** 8 m.
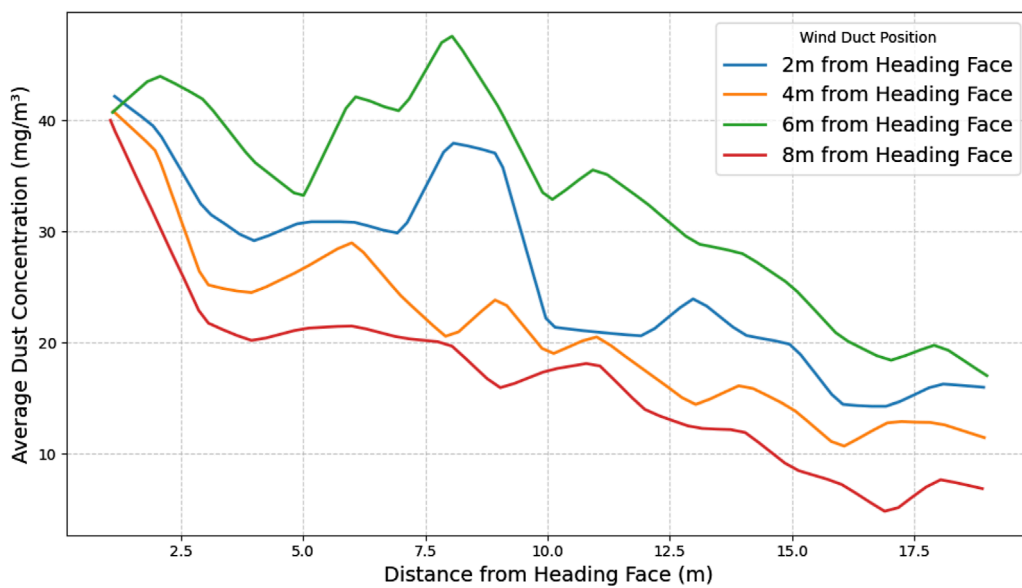


**FIGURE 9**
Average dust concentration distribution across the roadway cross-section at different distances between the air duct outlet and the working face.
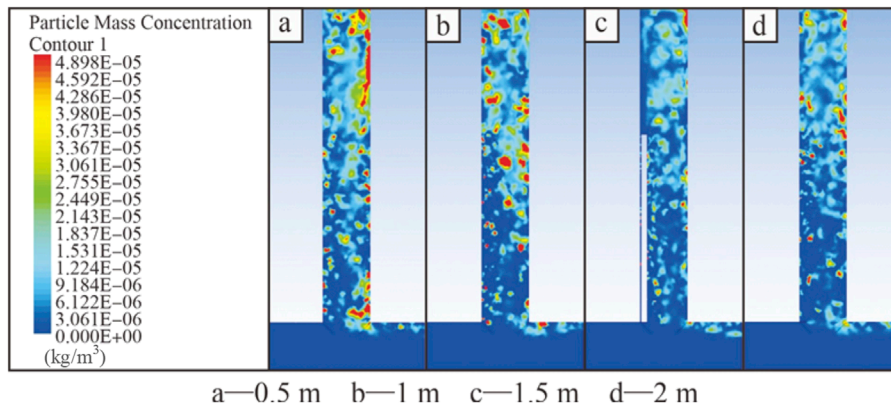
**FIGURE 10**
Dust concentration distribution at the working face for different air duct heights. **(A)** 0.5 m **(B)** 1 m **(C)** 1.5 m **(D)** 2 m.
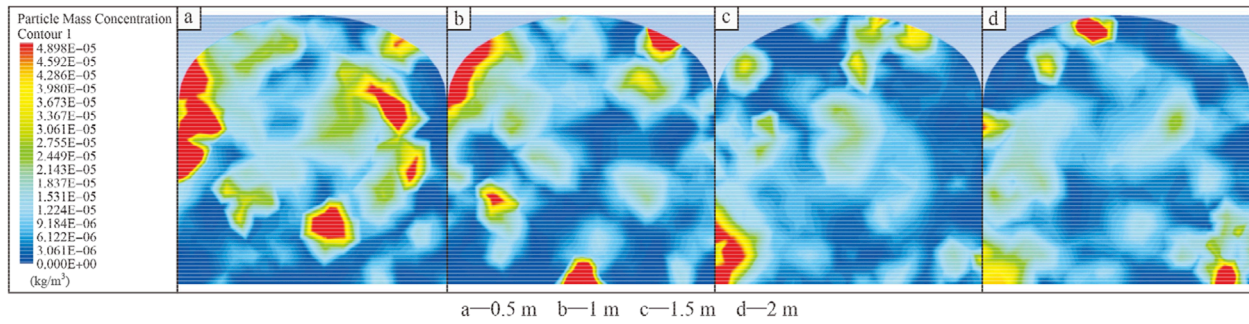


**FIGURE 11**
Dust concentration distribution at 3 m from the working face for different ventilation duct heights. **(A)** 0.5 m **(B)** 1 m **(C)** 1.5 m **(D)** 2 m.



**FIGURE 12**
Average dust concentration distribution across the roadway cross-section for different duct heights.

# 6 Conclusion

This study investigated dust transport behavior during tunneling operations and examined the effects of different air duct arrangements on dust control through numerical simulations. By focusing on varying duct outlet distances and heights, the study identified optimal configurations to minimize dust concentration and enhance worker safety.

(1) The results showed that positioning the air duct outlet 8 m from the working face significantly reduced dust concentration, achieving an average dust concentration of approximately 39 mg/m³. Additionally, setting the air duct height at 1.5 m proved to be the most effective in reducing dust levels in the worker breathing zone, highlighting the critical role of precise duct placement in dust control.

(2) The novelty of this research lies in its application of detailed numerical simulations to systematically evaluate and optimize ventilation configurations in underground tunneling environments. The use of grid independence verification ensured accuracy while maintaining computational efficiency, providing a robust framework for assessing ventilation system performance.

(3) These findings offer practical guidance for improving mine ventilation system design and contribute to the development of safer and healthier underground working environments. Future research could focus on integrating experimental validation and exploring the influence of dynamic working conditions and irregular tunnel geometries to further enhance the applicability of these results.

## Data availability statement

The original contributions presented in the study are included in the article/supplementary material, further inquiries can be directed to the corresponding author.

## Author contributions

YL: Data curation, Formal Analysis, Investigation, Resources, Software, Supervision, Writing–original draft, Writing–review and editing. JW: Conceptualization, Data curation, Formal Analysis, Funding acquisition, Methodology, Software, Supervision, Visualization, Writing–original draft, Writing–review and editing. ZL: Data curation, Formal Analysis, Investigation, Methodology, Software, Writing–review and editing. HM: Funding acquisition, Investigation, Resources, Software, Supervision, Writing–original draft.

## Conflict of interest

Authors ZL and HM were employed by China Coal Technology and Engineering Group Corp.

The remaining authors declare that the research was conducted in the absence of any commercial or financial relationships that could be construed as a potential conflict of interest.

## Generative AI statement

The author(s) declare that no Generative AI was used in the creation of this manuscript.

## Publisher's note

All claims expressed in this article are solely those of the authors and do not necessarily represent those of their affiliated organizations, or those of the publisher, the editors and the reviewers. Any product that may be evaluated in this article, or claim that may be made by its manufacturer, is not guaranteed or endorsed by the publisher.

## References

Abbasi, B., Wang, X., Chow, J. C., Watson, J. G., Peik, B., Nasiri, V., et al. (2021). Review of respirable coal mine dust characterization for mass concentration, size distribution and chemical composition. *Minerals* 11 (4), 426. doi:10.3390/min11040426

Chen, X., Zhang, H., Ge, S., Deng, C., Fan, C., Ma, G., et al. (2022). Research on the dust diffusion and pollution behaviour of dynamic tunneling in header excavators based on dynamic mesh technology and field measurement. *Energies* 15 (23), 8945. doi:10.3390/en15238945

Du, T., Nie, W., Chen, D., Xiu, Z., Yang, B., Liu, Q., et al. (2020). CFD modeling of coal dust migration in an 8.8-meter-high fully mechanized mining face. *Energy* 212, 118616. doi:10.1016/j.energy.2020.118616

Geng, T., Chen, K., and Huang, X. (2021). Study on dump truck dumping process and dust extraction device design Journal of Physics: conference Series. *IOP Publ.* 1885 (4), 042028. doi:10.1088/1742-6596/1885/4/042028

Hu, S., Liao, Q., Feng, G., Huang, Y., Shao, H., Gao, Y., et al. (2020). Influences of ventilation velocity on dust dispersion in coal roadways. *Powder Technol.* 360, 683–694. doi:10.1016/j.powtec.2019.09.080

Jing, D., Jiang, Z., Ma, M., Zhang, T., Liu, H., and Yu, T. (2022a). Study on dust migration law and spray dedusting technology in parallel double belt transportation. *Sci. Rep.* 12 (1), 5361. doi:10.1038/s41598-022-09200-1

Jing, D., Liu, H., Zhang, T., Ge, S., Ren, S., and Ma, M. (2022b). Study on coal dust diffusion law and new pneumatic spiral spray dedusting technology at transfer point of mine cross roadway. *PLoS one* 17 (8), e0272304. doi:10.1371/journal.pone.0272304

Khan, A. M., Ray, S. K., Mohalik, N. K., Mishra, D., Mandal, S., and Pandey, J. K. (2022). Experimental and CFD simulation techniques for coal dust explosibility: a review. *Min. Metallurgy and Explor.* 39 (4), 1445–1463. doi:10.1007/s42461-022-00631-y

Kurnia, J. C., Sasmito, A. P., and Mujumdar, A. S. (2014). Simulation of a novel intermittent ventilation system for underground mines. *Tunn. Undergr. Space Technol.* 42, 206–215. doi:10.1016/j.tust.2014.03.009

Liu, F., and Feng, X. (2021). Study on dust concentration distribution in a construction tunnel. *IOP Conf. Ser. Earth Environ. Sci.* 687 (1), 012162. doi:10.1088/1755-1315/687/1/012162

Liu, T., and Liu, S. (2020). The impacts of coal dust on miners' health: a review. *Environ. Res.* 190, 109849. doi:10.1016/j.envres.2020.109849

Lu, X., Wang, C., Xing, Y., Shen, C., and Shi, G. y. (2021). Investigation on the dust migration behavior and safety zone in the fully mechanized mining face. *Environ. Sci. Pollut. Res.* 28, 20375–20392. doi:10.1007/s11356-020-12050-x

Önder, M., Önder, S., Akdag, T., and Ozgun, F. (2009). Investigation of dust levels in different areas of underground coal mines. *Int. J. Occup. Saf. Ergonomics* 15 (1), 125–130. doi:10.1080/10803548.2009.11076794

Perret, J. L., Plush, B., Lachapelle, P., Hinks, T. S., Walter, C., Clarke, P., et al. (2017). Coal mine dust lung disease in the modern era. *Respirology* 22 (4), 662–670. doi:10.1111/resp.13034

Shekarian, Y., Rahimi, E., Rezaee, M., Su, W. C., and Roghanchi, P. (2021). Respirable coal mine dust: a review of respiratory deposition, regulations, and characterization. *Minerals* 11 (7), 696. doi:10.3390/min11070696

Trechera, P., Moreno, T., Córdoba, P., Moreno, N., Zhuang, X., Li, B., et al. (2021). Comprehensive evaluation of potential coal mine dust emissions in an open-pit coal mine in Northwest China. *Int. J. Coal Geol.* 235, 103677. doi:10.1016/j.coal.2021.103677

Wu, L., Chen, H., Li, J., Fu, S., and Zhuang, Y. (2021). Dust concentration changing regularities and dust reduction technology by spray negative pressure in fully mechanized mining face. *Geofluids* 2021 (1), 1–16. doi:10.1155/2021/1391673

Xiu, Z., Nie, W., Yan, J., Chen, D., Cai, P., Liu, Q., et al. (2020). Numerical simulation study on dust pollution characteristics and optimal dust control air flow rates during coal mine production. *J. Clean. Prod.* 248, 119197. doi:10.1016/j.jclepro.2019.119197

Yang, J., Qiao, B., Gao, Y., Gao, H., Wei, X., and Fu, Q. (2021). Study on the gas migration laws of non-pillar mining with gob-side entry retaining in high gas

outburst coal seam. *IOP Conf. Ser. Earth Environ. Sci.* 861 (5), 052058. doi:10.1088/1755-1315/861/5/052058

Zeqiri, I., Gashi, J., Brahimaj, F., and Zeqiri, R. (2022). Effectiveness of ventilation regulation in a simple diagonal system of underground mines. *Min. Mineral Deposits* 16 (2), 81–86. doi:10.33271/mining16.02.081

Zhang, G., Sun, B., Song, S., Wang, H., and Zhou, G. (2021). CFD comparative analysis on the pollution characteristics of coal dust under turbulent airflow from coal cutting in the fully mechanized mining face. *Process Saf. Environ. Prot.* 146, 515–530. doi:10.1016/j.psep.2020.11.044

Zhang, J., Han, Z., Chen, T., Yao, N., Yang, X., Chen, C., et al. (2024). A numerical simulation of the coal dust migration law in directional air drilling in a broken soft coal seam. *Processes* 12 (2), 309. doi:10.3390/pr12020309

Zhao, J., Gao, G., and Gao, X. (2024). Study on the influence of dust removal fan structure parameters on dust removal performance. *Appl. Sci.* 14 (8), 3405. doi:10.3390/app14083405

Zhou, G., Cheng, W., Zhang, R., Shen, B. t., Nie, W., Zhang, L., et al. (2015). Numerical simulation and disaster prevention for catastrophic fire airflow of main air-intake belt roadway in coal mine—a case study. *J. Central South Univ.* 22, 2359–2368. doi:10.1007/s11771-015-2761-x

Zhou, G., Jing, B., Meng, Q., Liu, Y., Yang, W., and Sun, B. (2023). Study on coupling diffusion of composite dust and cloud-mist dedust technology in fully mechanized driving face of mixed coal-rock roadway. *Adv. Powder Technol.* 34 (1), 103911. doi:10.1016/j.apt.2022.103911

Zhou, G., Liu, Y., Kong, Y., Hu, Y., Song, R., Tian, Y., et al. (2022). Numerical analysis of dust pollution evolution law caused by ascensional/descensional ventilation in fully mechanized coal mining face based on DPM-DEM model. *J. Environ. Chem. Eng.* 10 (3), 107732. doi:10.1016/j.jece.2022.107732

Zhou, G., Zhang, Q., Bai, R., Fan, T., and Wang, G. (2017). The diffusion behavior law of respirable dust at fully mechanized caving face in coal mine: CFD numerical simulation and engineering application. *Process Saf. Environ. Prot.* 106, 117–128. doi:10.1016/j.psep.2016.12.005